Environmental Research Letters

LETTER

# Roles of interbasin frequency changes in the poleward shifts of the maximum intensity location of tropical cyclones

**Il-Ju Moon**[1], **Sung-Hun Kim**[1], **Phil Klotzbach**[2] **and Johnny C L Chan**[3]

[1] Typhoon Research Center, Jeju National University, Ara 1 Dong. Jejusi 690-756, Korea
[2] Department of Atmospheric Science, Colorado State University, Fort Collins, CO 80523, USA
[3] Guy Carpenter Asia-Pacific Climate Impact Centre, School of Energy and Environment, City University of Hong Kong, Hong Kong

**E-mail:** waterneedskim@gmail.com

**Keywords:** tropical cyclone, poleward migration, maximum intensity location, frequency change

Supplementary material for this article is available online

OPEN ACCESS

RECEIVED
20 July 2015

REVISED
9 September 2015

ACCEPTED FOR PUBLICATION
10 September 2015

PUBLISHED
6 October 2015

Content from this work may be used under the terms of the Creative Commons Attribution 3.0 licence.

Any further distribution of this work must maintain attribution to the author(s) and the title of the work, journal citation and DOI.

## Abstract

An observed poleward migration in the average latitude at which tropical cyclones (TCs) achieved their lifetime-maximum intensities (LMIs) was previously explained by changes in the mean meridional environments favorable to storm development linked to tropical expansion and anthropogenic warming. We show that the poleward migration is greatly influenced by basin-to-basin changes in TC frequency associated with multi-decadal variability, particularly for the Northern Hemisphere (NH). The contribution of the frequency changes to the poleward migration is comparable to that of the mean meridional environmental changes. A statistically significant global poleward trend can be identified simply from the frequency changes in each basin. An opposite trend exists in the frequency variations over the past 30 years between the North Atlantic and the eastern North Pacific where climatological mean latitudes of LMI are high (26.1°N) and low (16.5°N), respectively, which is the key factor in driving the frequency contribution. The strong roles of the interbasin frequency changes in the poleward migration also suggest that if the phase of multidecadal variability in the NH is reversed, as found in earlier TC records, the poleward trend could be changed to an opposite, equatorward, trend in the future.

## 1. Introduction

Recent catastrophic events such as Cyclone Nargis (2008), Hurricane Sandy (2012), and Supertyphoon Haiyan (2013) have led scientists to ask how climate change is affecting tropical cyclone (TC) behavior (Kang and Elsner 2015). Particularly, considerable attention has been devoted to poleward shifts in the geographical location at which the lifetime-maximum intensities (LMIs) of storms occur (Kossin *et al* 2014, hereafter, KEV), in addition to changes in TC intensity and frequency (Maue 2011). The observed shifts of LMI towards the poles are 53 and 62 Km per decade in the Northern Hemisphere (NH) and the Southern Hemisphere (SH), respectively over the past three decades. This result implicitly implies that TCs moving along similar tracks will experience their LMI at higher latitudes than before, which potentially increases threats to coastal cities at higher latitudes that have historically not been as prone to strong TC impacts (Ramsay 2014). KEV proposed that such a poleward migration is linked to marked changes in the mean meridional structure of environmental vertical wind shear and potential intensity due to tropical expansion and anthropogenic warming (KEV).

Despite the pronounced and statistically significant global and hemispheric mean trends in poleward migration, the trends in each basin are mostly insignificant in KEV. For example, five out of six basins show insignificant trends on the basis of historical 'best-track' data (see table 1 of KEV). Particularly for the North Atlantic (NA), which has seen a marked increase in TC activity since the mid-1990s, there is almost no poleward trend over the past 30 years (Ramsay 2014). Although it turns out that the trends in individual basins vary depending on TC data sources and analysis methods (see supporting information S1), the large discrepancy between the regional and global (or

© 2015 IOP Publishing Ltd

hemispheric) trends in KEV raises the question as to how a statistically significant global mean trend can occur without significant trends in most basins. In this paper, we perform a quantitative analysis to identify the contributions to the trends and attempt to determine whether the observed poleward trend of LMI latitude will continue.

This paper consists of six sections. Data and methods are introduced in section 2. Section 3 describes trends in annual-mean latitudes of LMI in each basin as well as for the global/hemispheric mean. Section 4 investigates factors contributing to the poleward trend through a quantitative analysis. Results are discussed in section 5, while a summary and conclusion are given in section 6.

## 2. Data and methods

Global best track data were obtained from the International Best Track Archive for Climate Stewardship (IBTrACS, version v03r05) (Knapp *et al* 2010). We use IBTrACS-ALL data in which the best track data were provided by all agencies and dataset sources, since IBTrACS-WMO data provided only from WMO-sanctioned forecast agencies has missing data in the North Indian Ocean before 1990. When a storm has overlapping data from multiple sources, we use the source with the greatest reported LMI as in KEV. For storms that achieve their LMI more than once, the latitude of LMI is taken at the first occurrence. For TCs passing the International Date Line in the Pacific, the ocean basin to which the TC belongs is determined according to the location where the storm reached its LMI. Significance tests on linear trends are conducted using the Mann–Kendall trend test (Mann 1945, Kendall 1970).

The annual global-mean latitude of LMI $\left(\overline{\mathrm{LLMI}}_{\mathrm{global}}\right)$ is determined by the sum of multiplying the annual-mean LMI latitude ($\overline{\mathrm{LLMI}}_{\mathrm{basin}}$) for each basin by the ratio of annual TC frequency ($N_{basin}$) for each basin to the total global TC frequency ($N_{\mathrm{global}}$) in all basins. Here the annual-mean latitude of LMI ($\overline{\mathrm{LLMI}}_{\mathrm{basin}}$) can be divided into two components: climatological-mean LMI latitude ($\overline{\mathrm{LLMI}}_{\mathrm{Clim}_{\mathrm{basin}}}$) and anomaly ($\Delta\overline{\mathrm{LLMI}}_{\mathrm{basin}}$) from the mean value for each basin:

$$\begin{aligned}\overline{\mathrm{LLMI}}_{\mathrm{global}} &= \sum_{\mathrm{basin}}\left(\overline{\mathrm{LLMI}}_{\mathrm{basin}} \times \frac{N_{\mathrm{basin}}}{N_{\mathrm{global}}}\right), \\ &= \sum_{\mathrm{basin}}\left(\overline{\mathrm{LLMI}}_{\mathrm{Clim}_{\mathrm{basin}}} \times \frac{N_{\mathrm{basin}}}{N_{\mathrm{global}}}\right) \\ &\quad + \sum_{\mathrm{basin}}\left(\Delta\overline{\mathrm{LLMI}}_{\mathrm{basin}} \times \frac{N_{\mathrm{basin}}}{N_{\mathrm{global}}}\right). \quad (1)\end{aligned}$$

Hemispheric-mean LMI latitude can be calculated in the same manner using total TC frequency ($N_{\mathrm{HEMI}}$) in each hemisphere instead of $N_{\mathrm{global}}$.

The Nino-3.4 index (Barnston *et al* 1997) that is used to reduce the contribution of El Niño/Southern oscillation (ENSO) is the average of the monthly values during the most active TC periods of each hemisphere (August–October in the NH and January–March in the SH). The Atlantic multidecadal oscillation (AMO) index is calculated from the Kaplan sea surface temperature (SST) dataset (Enfield *et al* 2001). The Pacific decadal oscillation (PDO) index is derived as the leading principle component of monthly SST anomalies in the North Pacific Ocean (Mantua *et al* 1997). Vertical wind shears (200–850 hPa) for the NA and the Eastern Pacific (EP) are averaged over the main development regions (EP, 10–20°N, 220–265°E; NA, 10–20°N, 280–340°E, 20–30°N, 265–310°E) during the TC peak season (July–October) using the NCEP/NCAR reanalysis (Kistler *et al* 2001).

## 3. Trends in annual-mean latitudes of LMI

The annual-mean latitudes of LMI for the NH, SH, global, and interhemispheric span (IS) (the global migration of the latitude of LMI away from the tropics) are extracted from the global best-track data for the 31-year period 1982–2012 (figure 1). Here the calculation has been done for TCs that are of at least tropical storm intensity (see supporting information S1). Since changes in TC tracks and frequencies in most regions have been linked to phase changes in ENSO (Camargo *et al* 2007, Chan 2000), we decrease the contribution of ENSO for each basin by regressing the time series of both the LMI latitude and frequency onto an index of ENSO variability and analyzing the residuals (dashed lines in figure 2). Using the multiple of the two residuals of the regression (see equation (1)), we obtain the poleward trends of LMI locations with rates of 52, 55, 58 and 107 km per decade in the NH, SH, global, and IS respectively (green straight lines in figure 1; table 1), which are all statistically significant with 95% confidence and similar to those of KEV. A similar calculation without reducing the ENSO contribution (figure 1, black lines) gives rates of 60, 55, 62 and 115 km per decade, respectively. The small differences between the two calculations suggest that ENSO plays only a minor role in the long-term hemispheric and global trends of the LMI latitude, as reported in KEV.

Compared to the hemispheric or global mean trends (significant at 99%), the trends in individual ocean basin are not robust (figure 2(a), table 1). In particular, in the NH that accounts for 68% of global TC frequency (table 1), negative contributions are found from the NA and the North Indian Ocean, although they are not statistically significant. The negative contributions were also shown by KEV in their table 1 using a different dataset. The discrepancy in the annual-mean trends between the NH (or global) and the individual basins is a result of the contribution of the temporal variations in the relative annual

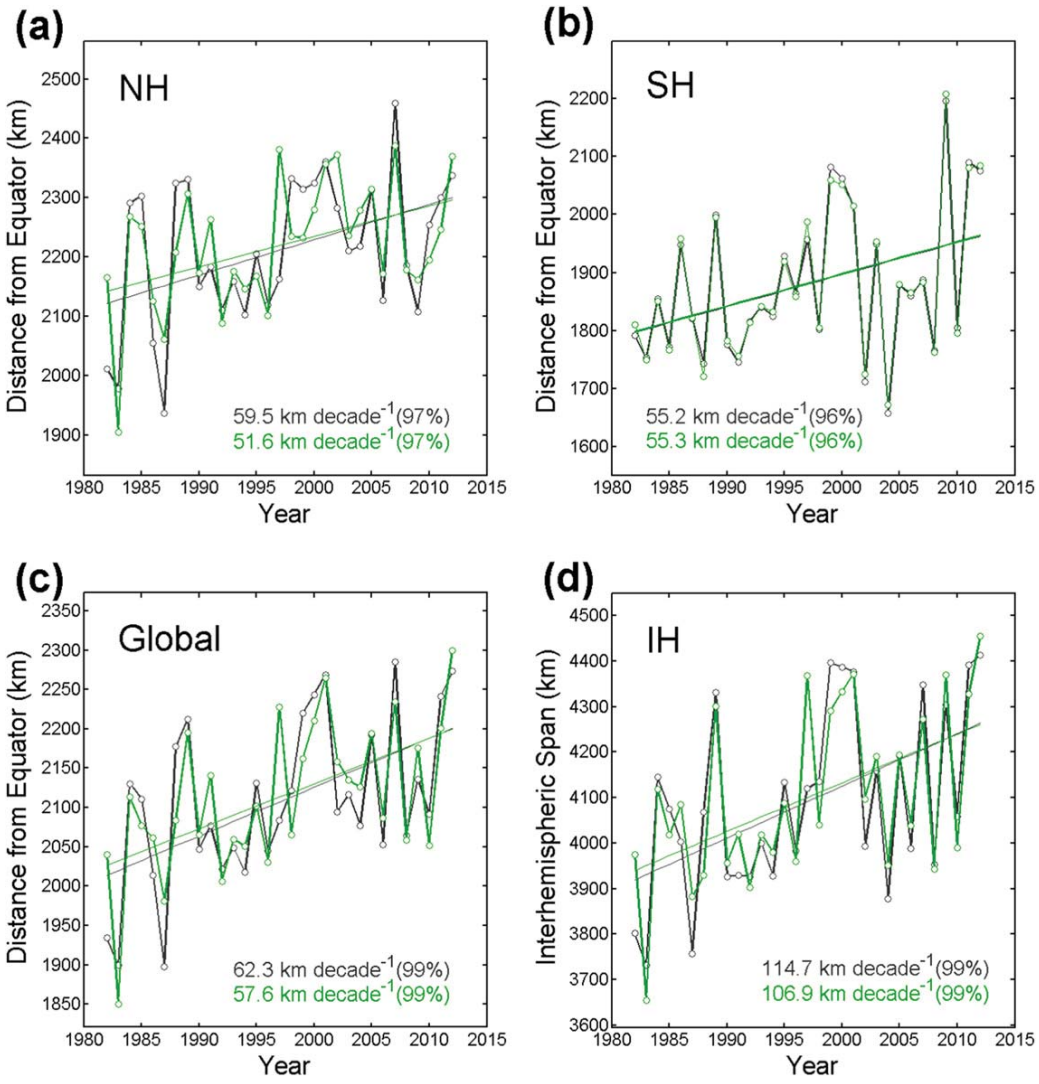


**Figure 1.** Time series of annual-mean latitude of tropical cyclone LMI and linear trends (straight lines) representing poleward migrations of the LMI latitude away from the equator for (a) the NH, (b) SH, (c) global, and (d) interhemispheric span. Black colors represent the original time series and green lines represent the time series with ENSO variability reduced. Linear trends of each time series are shown with their significance levels (in parentheses).

frequency of storms from each basin where climatological mean LMI latitude is greatly different (figure 2(b), table 1). The trends in the percentage of the annual TC frequency for each basin to the total annual global TC frequency are clear and statistically significant at a 95% confidence level in all basins of the NH except the western North Pacific where the trend is only significant at 72% confidence (table 1). Climatological mean latitudes of LMI are in the range from 15.9°N to 26.1°N for the four NH basins. It is noted that the NA, with the highest LMI latitude (26.1°N), and the eastern North Pacific, with the second lowest LMI latitude (16.5°N), have a strong opposite trend in the variations of TC frequency (table 1, figure 2(b)). These two basins comprise 47% of the total TC frequency in the NH and historically have an out-of-phase relationship to each other in TC activity for both interannual and multidecadal variability (Wang and Lee 2009, Wang and Lee 2010). It turns out that the frequency trends in the two basins strongly affect the poleward trend of the LMI location in the NH, which will be investigated in the next section.

## 4. Contributions of TC frequency to the poleward trends

On the basis of equation (1), the contributions of the global poleward trends can be divided into two components. The first term on the right-hand-side of equation (1) represents the trend by changes in the relative annual TC frequency from each basin (hereafter, the frequency contribution) since the annual-mean latitude of LMI at each basin is fixed to the climatological values and only the frequency part

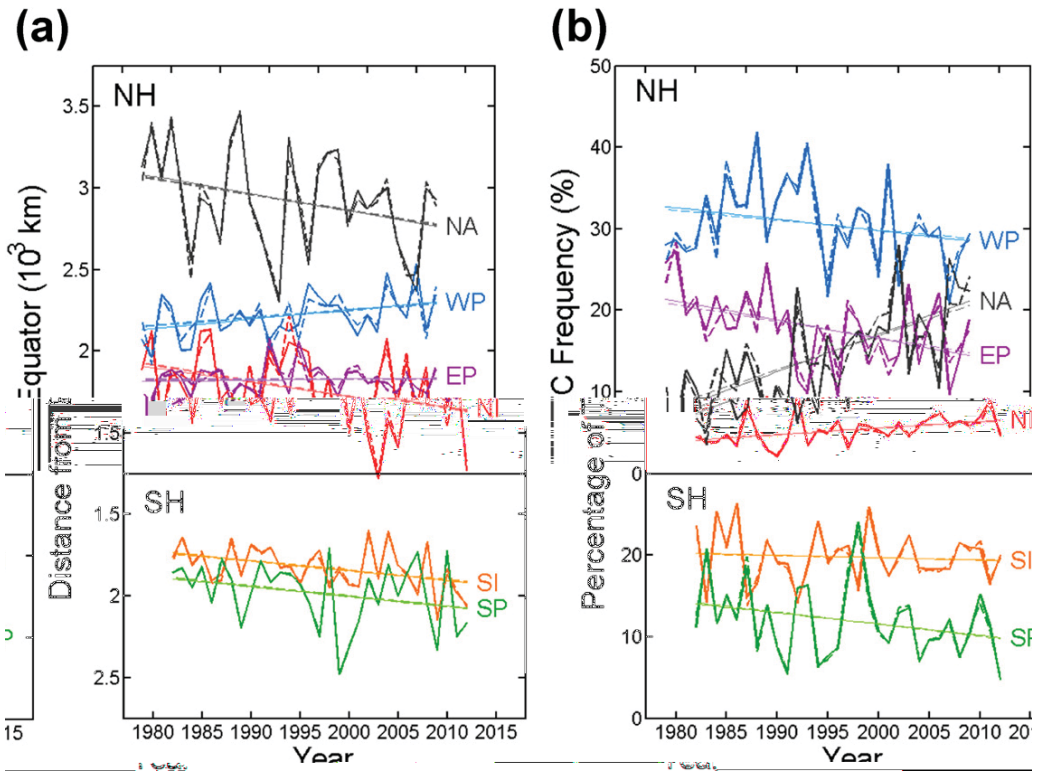


**Figure 2.** Time series of (a) annual-mean latitude of LMI and (b) percentages of TC frequency to the total global TC frequency and their linear trends (straight lines) from each ocean basin. Dashed lines represent the time series with ENSO variability removed. Linear trends of each time series are shown in table 1 with their significance levels. The basins are the North Atlantic (NA), the western North Pacific (WP), the eastern North Pacific (EP), the northern Indian Ocean (NI), the southern Indian Ocean (SI) and the South Pacific (SP). Note that the *y* axis in the SH of (a) increase downwards.

changes annually. The second term represents the trend by the pure poleward migration of LMI latitude at each basin (hereafter, the pure migration contribution) since the contributions of the TC frequency are removed by the normalization using the anomaly. The sum of these two contributions is then the total trend of annual-mean migration of LMI latitude for each basin as well as for the hemisphere or global mean. This method of separating the trends into two components allows a quantitative estimation of the relative contribution of each component to the trends.

For the two components, the analysis of figure 1(a) is repeated. When this was done, it is clear that the trend in the NH is mainly determined by the frequency contribution (figure 3(a)) while that in the SH is mostly controlled by the pure migration contribution (figure 3(b)). In the NH, 92% (47.7 km per decade) of the poleward trend of 51.6 km per decade is a result of the frequency contribution, and only 8% (3.9 km per decade) is from the pure poleward migration contribution within each basin. In the SH, 59.5 km per decade is from the pure migration contribution and −4.1 km per decade is from the frequency contribution. In terms of the global average and the IS, the frequency contribution overwhelms the poleward trends since the NH accounts for the majority (68%) of the global TC frequency. This is well demonstrated by the fact that a statistically significant poleward trend of LMI migration with 99% confidence is produced by using only the frequency contribution for both the global average and IS (figures 3(c) and (d)).

To quantify the frequency contributions from each ocean basin, the linear trend analysis is repeated using the following annual residuals for each basin

$$\text{Annual residual}_{\text{basin}} = \Big( \Big( \big( N_{\text{basin}} - \overline{N}_{\text{Clim}_{\text{basin}}} \big) \times \big( \overline{\text{LLMI}}_{\text{Clim}_{\text{basin}}} - \overline{\text{LLMI}}_{\text{Clim}_{\text{global}}} \big) \Big) / \big( N_{\text{global}} \big) \Big), \quad (2)$$

where $N_{\text{basin}}$, $N_{\text{global}}$, $\overline{N}_{\text{Clim}_{\text{basin}}}$, $\overline{\text{LLMI}}_{\text{Clim}_{\text{basin}}}$, and $\overline{\text{LLMI}}_{\text{Clim}_{\text{global}}}$ are annual TC frequency for each basin, annual global TC frequency, climatological basin-mean TC frequency, climatological basin-mean latitude of LMI, and climatological global-mean latitude of LMI, respectively. This analysis provides an estimate of how much of the trends for each individual basin contributes to the global poleward trends (36.9 km per decade of figure 3(c)) due to the frequency contribution. The analysis reveals that the frequency changes in the NA and the EP are leading most of the frequency contribution shown in the global mean trend (table 1).

**Table 1.** Linear trends and climatological-mean values, by region, of annual-mean latitude of LMI and percentage of annual TC frequency for each basin to the total annual global TC frequency from 1982–2012. Trends are estimated from time series with ENSO variability reduced. Linear trends are shown with their significance levels in parentheses. Positive slopes in the latitude of LMI represent poleward migration. Bold-faced font represents that the trends are significant with more than 95% confidence. The linear trends by only the frequency contribution are estimated using residuals of equation (2).

| | WP | NA | EP | NI | SI | SP | NH | SH | GLB | IH |
|---|---|---|---|---|---|---|---|---|---|---|
| Linear trend of LMI latitude (km decade$^{-1}$) | 47.2 (93%) | −97.7 (88%) | 1.4 (1%) | −97.3 (94%) | 58.3 (97%) | 61.3 (82%) | 51.6 (97%) | 55.3 (96%) | 57.6 (99%) | 106.9 (99%) |
| Clim.-mean latitude of LMI | 20.1°N | 26.1°N | 16.5°N | 15.9°N | 16.5°S | 18.0°S | 20.1°N | 17.0°S | 19.1 | — |
| Linear trend of frequency percentage (% decade$^{-1}$) | −1.2 (72%) | 4.2 (99%) | −2.0 (97%) | 0.8 (99%) | −0.2 (16%) | −1.5 (80%) | 1.7 (87%) | −1.7 (87%) | — | — |
| Clim.-mean frequency percentage (%) | 30.6 | 14.4 | 17.9 | 5.4 | 19.8 | 12.0 | 68.2 | 31.8 | — | — |
| Linear trends by frequency contribution (km decade$^{-1}$) | −2.7 | 30.7 | 6.7 | −1.8 | 2.0 | 2.0 | 32.9 | 4.0 | 36.9 | |

Note. WP, western North Pacific; NA, North Atlantic; EP, eastern North Pacific; NI, North Indian Ocean; SI, South Indian Ocean; SP, South Pacific; NH, Northern Hemisphere; SH, Southern Hemisphere; GLB, global; IH, Interhemispheric Span.

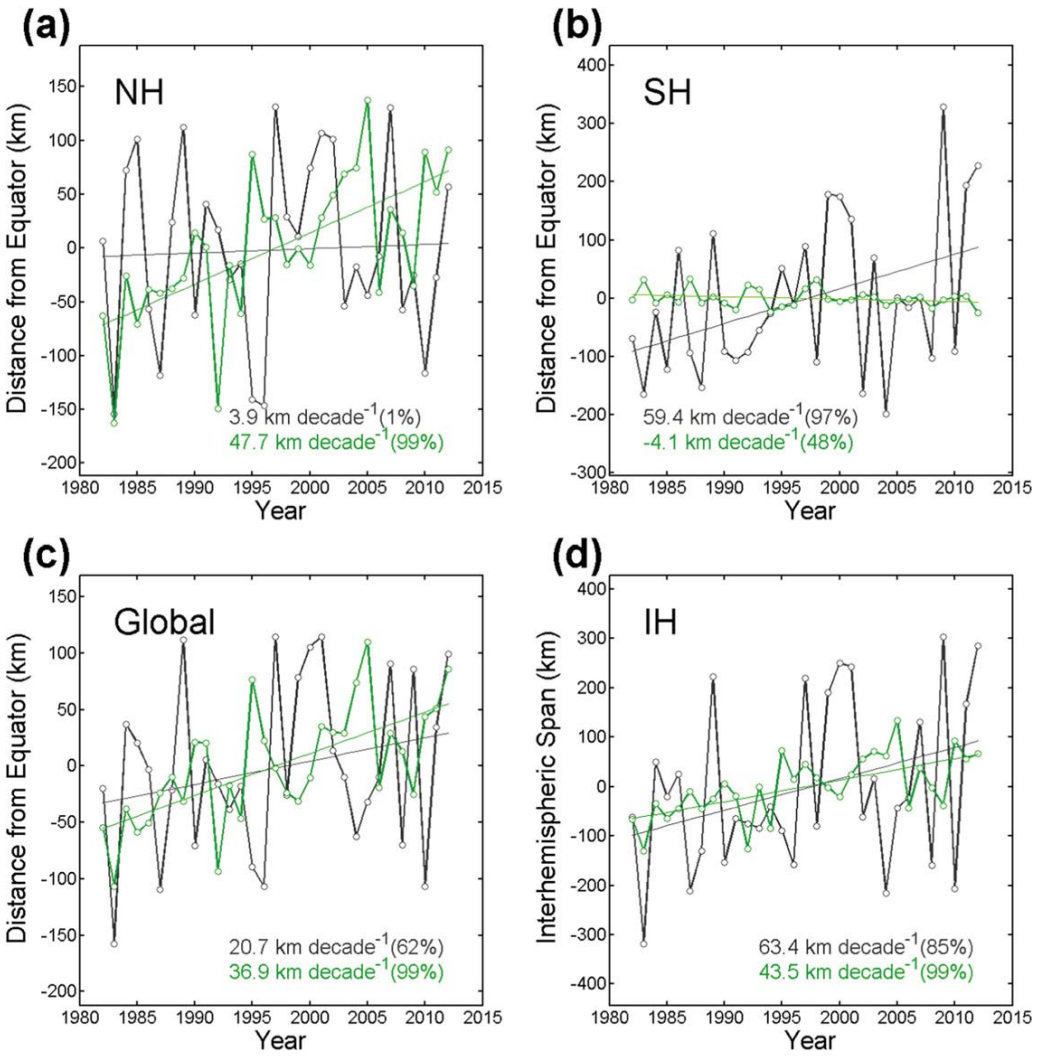


**Figure 3.** Time series of annual-mean latitude of tropical cyclone LMI by frequency contribution (green color) and pure migration contribution (black color) and their linear trends (straight lines) in (a) the NH, (b) SH, (c) global, and (d) interhemispheric span. Linear trends of each time series are shown with their significance levels (in parentheses). In all the time series, the effects of ENSO were reduced.

Based on these results, if we simply adjust the climatological-mean LMI latitudes for the two basins (NA: 26.1°N, EP: 16.5°N) to the global-mean (19.1°) or NH-mean (20.1°N) LMI latitude and keep the annual variability to remove the frequency contributions from the two basins, the poleward trend of annual-mean LMI latitude is no longer statistically significant (at least at a 90% confidence level) for the NH, globe, or IS (figure 4). These results suggest that an increasing trend of the relative annual-mean TC frequency in the NA (FRQ_NA) where the climatological mean LMI latitude is the highest and a decreasing trend of the frequency in the EP (FRQ_EA) where the mean LMI latitude is low is the main reason for the poleward trend of LMI latitude in the NH, which also influences global and IS trends.

The TC frequencies in the NA and EP, which have just been shown to be a key factor in the recent global poleward migration of LMI latitude, are well known to be linked not only to the interannual ENSO variability but also to decadal or longer climate variability such as the AMO and PDO (Delworth and Mann 2000, Chylek and Lesins 2008, Maue 2011, Grassi *et al* 2012). Using an extended data set (1953–2012), the multidecadal variations of TC FRQ_NA and the EP (FRQ_EA) are found to be highly correlated with the AMO ($r = 0.9$, AMO and FRQ_NA, where $r$ denotes the correlation coefficient) and the PDO ($r = 0.8$, PDO and FRQ_EA), respectively, which are both significant with 99% confidence (figure 5(a)). It is also shown that the AMO and PDO are linked to variations of the vertical wind shear (VWS) over the main TC development regions of the NA (VWS_NA) and EP (VWS_EP), respectively (figure 5(b)), which is a critical factor determining likelihood of TC genesis (Kossin

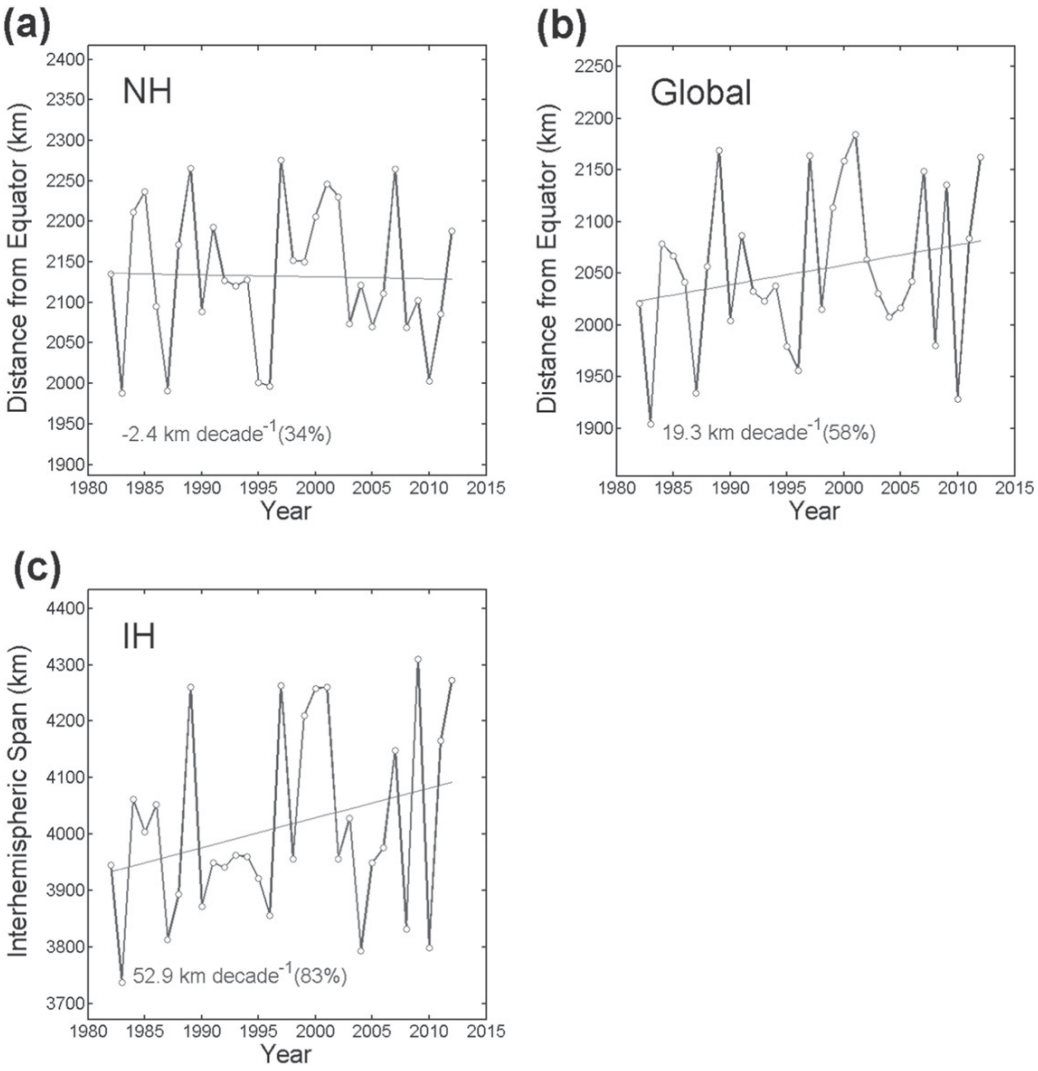


**Figure 4.** Migration trends of the LMI latitude for (a) NH, (b) global, and (c) interhemispheric span after removal of the frequency contributions in the North Atlantic (NA) and the eastern North Pacific (EP) by adjusting the climatological mean LMI latitudes for the two basins (NA: 26.1°N, EP: 16.5°N) to the global-mean (19.1°) or NH-mean (20.1°N) LMI latitude and keeping the annual variability. Linear trends of each time series are shown with their significance levels (in parentheses). In all the time series, the effects of ENSO were reduced.

*et al* 2010). These linkages imply that the poleward migration of the global LMI location observed during the last 30 years, at least in the NH, can be explained as part of a phase of such multidecadal variability. The close relationship between the (FRQ_NA)/FRQ_EA and the migration of LMI latitude is also found in the earlier data (figures 5(c) and (d)) although the data quality of the period could be an issue (Landsea *et al* 2010). During the earlier period (1953–1987), the frequency trends in the NA and the EP are opposite to those during the last 30 years, and the resulting trend of the global-mean LMI latitude is also reversed. This suggests that if the frequency trends in the two ocean basins are reversed, as found in earlier TC records, the NH poleward trend could be changed to an opposite, equatorward, trend in the future.

## 5. Discussions

KEV argued that the observed poleward migration trend of annual-mean LMI latitude is mainly caused by the marked changes in the mean meridional environments favorable to storm development linked to tropical expansion and anthropogenic warming. However, based on our quantitative analysis, the observed poleward migration is shown to be mostly controlled by interbasin changes in TC frequency, particularly for the NH. For the SH, the migration is controlled by the pure migration component for each basin, which means that there is a possibility that the poleward migration in the SH is influenced by the mean environmental changes such as vertical wind shear and potential intensity as suggested by KEV.

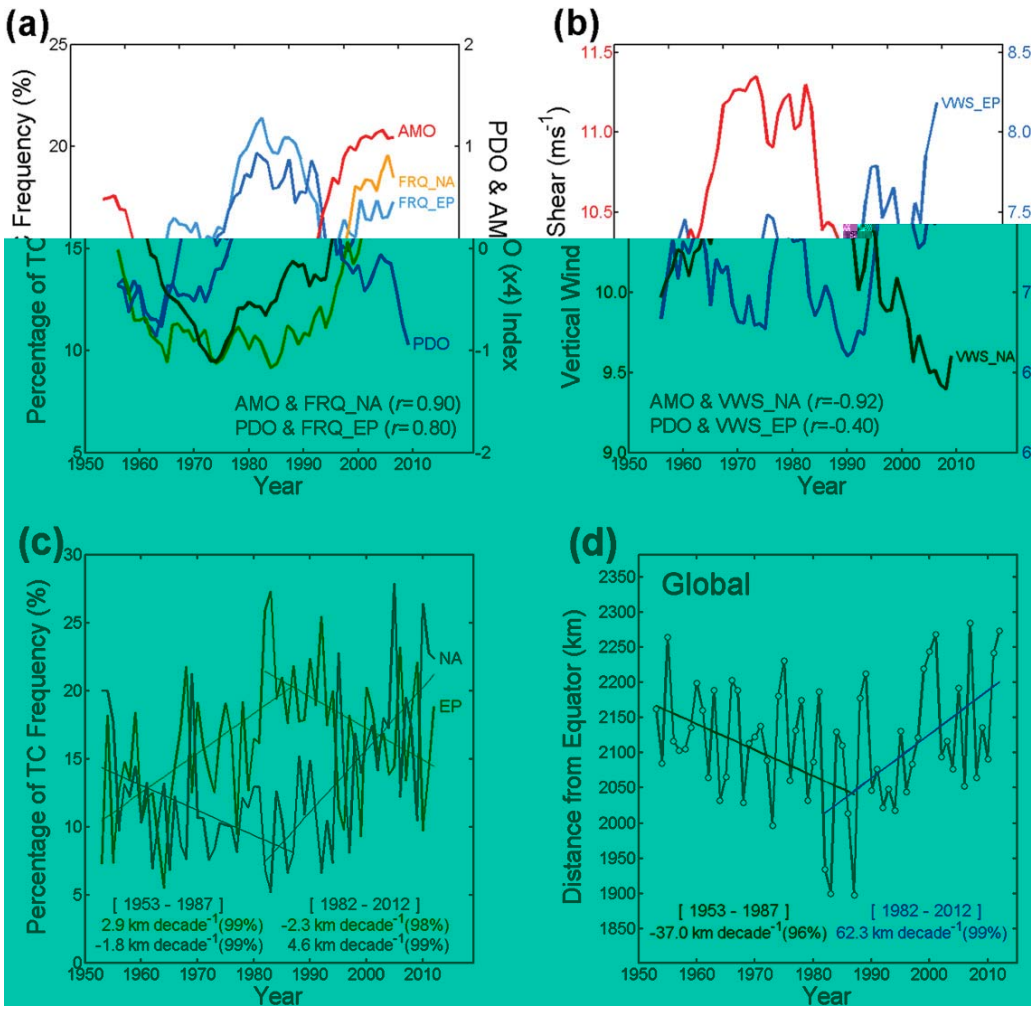


**Figure 5.** Connection among changes in relative annual TC frequency from the North Atlantic (NA) and the eastern North Pacific (EP), trends of latitude of LMI, and modes of climate variability: (a) time series of the AMO (red) index, PDO (blue) index, and percentages of TC frequency in the NA (dark yellow) and EP (light blue), which are obtained by performing a 7-year running mean after removal of the linear trend. (b) Time series of the 7-year running mean vertical wind shear (VWS) averaged over the main development regions of the NA (red) and EP (blue) during TC peak season (July–October). Correlation coefficients ($r$) among AMO, PDO, NA/EP (frequency and VWS) are denoted in the figures. (c) Time series of annual percentage of TC frequency in the NA (black color) and EP (green color) to total global TC frequency and their linear trends (straight lines) for two periods (1953–1987 and 1982–2012). (d) Time series of annual global-mean latitude of tropical cyclone LMI and two linear trends for earlier (red color) and a more recent (blue color) period. Each trend is shown with significance levels (in parentheses). All the trends are statistically significant with 95% confidence.

Why are the major causes of the poleward migration in both hemispheres different? One possible reason is the distinct geographical difference between the two hemispheres. In the NH, basin-to-basin differences in the annual TC frequency and climatological mean LMI latitudes are evident, probably due to a clear separation and disconnection between ocean basins by continent or different oceanic environments as well as due to different responses of each basin to various modes of climate variability (Camargo *et al* 2008, Kossin *et al* 2010, Holland and Bruyere 2013). Even in a basin of the NH, for example in the NA, the climatological mean LMI latitude and trend of TC frequency are different according to sub-basins such as the Gulf of Mexico, the Caribbean Sea, and the western NA. Therefore, the large changes at both intra-basin and inter-basin levels in the NH dominate the variability of the LMI latitude, leading to a hampering of ability to detect the trends of pure poleward migration in each basin of the NH. In the SH, the South Pacific and the South Indian Ocean are similar in terms of the variability of the climatological mean LMI latitude and TC frequency. In addition, the variability within each basin is not as large, which may lead to the clear detection of the pure poleward trend in the SH.

## 6. Summary and conclusions

A quantitative analysis of historical global TC track data reveals that the observed poleward migration of LMI latitude is largely influenced by basin-to-basin changes in TC frequency. Particularly for the NH which accounts for the majority of global TC frequency, 92% of the poleward trend is a result of the frequency changes. The linear trend analysis reveals that the recent increasing and decreasing trends of TC (FRQ_NA) and FRQ_EA, respectively, with high and low climatological mean LMI latitudes (NA = 26.1° N, EP = 16.5°N) play a key role in the poleward migration in the NH. The frequency contribution well illustrates how the global and hemispheric poleward trends become statistically significant in spite of the insignificant trends observed in most basins of the NH in KEV. Due to the dominance of the frequency control in the LMI latitudes in the NH, we could even produce a statistically significant global poleward trend only using interbasin frequency changes without any poleward migration in all basins. Additional analyses show that the TC frequencies and VWS (a major index related to TC genesis) in the NA and EP are highly correlated with decadal or longer climate variability such as the AMO and PDO. These imply that the poleward migration of the global LMI location observed during the last 30 years could be changed to an opposite trend in the future if the phase of multidecadal variability in the NH is reversed.

## Acknowledgments

This work has been performed as a subproject of KISTI's project 'Building Response System for National-wide Issues Based on High-performance Supercomputer'. The work of JCLC was supported by the Research Grants Council of the Hong Kong Special Administrative Region Grant CityU 100113.

## References

Barnston A G, Chelliah M and Goldenberg S B 1997 Documentation of a highly ENSO related SST region in the equatorial Pacific *Atmos.—Oceans* **35** 367–83

Camargo S J, Robertson A W, Barnston A G and Ghil M 2008 Clustering of eastern North Pacific tropical cyclone tracks: ENSO and MJO effects *Geochem. Geophys. Geosyst.* **9** Q06V05

Camargo S J, Robertson A W, Gaffney S J, Smyth P and Ghil M 2007 Cluster analysis of typhoon tracks: II. Large-scale circulation and ENSO *J. Clim.* **20** 3654–76

Chan J C L 2000 Tropical cyclone activity in the western North Pacific associated with El Niño and La Niña events *J. Clim.* **13** 2960–72

Chylek P and Lesins G 2008 Multidecadal variability of Atlantic hurricane activity: 1851–2007 *J. Geophys. Res.* **113** D22106

Delworth T L and Mann M E 2000 Observed and simulated multidecadal variability in the Northern Hemisphere *Clim. Dyn.* **16** 661–76

Enfield D B, Mestas-Nunez A M and Trimble P J 2001 The Atlantic multidecadal oscillation and its relation to rainfall and river flows in the continental US *Geophys. Res. Lett.* **28** 2077–80

Grassi B, Redaelli G, Canziani P O and Visconti G 2012 Effects of the PDO phase on the tropical belt width *J. Clim.* **25** 3282–90

Holland G and Bruyere C L 2013 Recent intense hurricane response to global climate change *Clim. Dyn.* **42** 617–27

Kang N-Y and Elsner J B 2015 Trade-off between intensity and frequency of global tropical cyclones *Nat. Clim. Change* **5** 661–4

Kendall M G 1970 *Rank Correlation Methods* 2nd edn (New York: Hafner)

Kistler R *et al* 2001 The NCEP-NCAR 50-year reanalysis: monthly means cd-rom and documentation *Bull. Am. Meteorol. Soc.* **82** 247–67

Knapp K R, Kruk M C, Levinson D H, Diamond H J and Neumann C J 2010 The International best track archive for climate stewardship (IBTrACS): unifying tropical cyclone data *Bull. Am. Meteorol. Soc.* **91** 363–76

Kossin J P, Camargo S J and Sitkowski M 2010 Climate modulation of North Atlantic hurricane tracks *J. Clim.* **23** 3057–76

Kossin J P, Emanuel K A and Vecchi G A 2014 The poleward migration of the location of tropical cyclone maximum intensity *Nature* **509** 349–52

Landsea C W, Vecchi G A, Bengtsson L and Knutson T R 2010 Impact of duration thresholds on Atlantic tropical cyclone counts *J. Clim.* **23** 2508–19

Mann H B 1945 Nonparametric tests against trend *Econometrica* **13** 245–59

Mantua N J, Hare S R, Zhang Y, Wallace J M and Francis R C 1997 A Pacific interdecadal climate oscillation with impacts on salmon production *Bull. Am. Meteorol. Soc.* **78** 1069–79

Maue R N 2011 Recent historically low global tropical cyclone activity *Geophys. Res. Lett.* **38** L14803

Ramsay H 2014 Shifting storms *Nature* **509** 290–1

Wang C and Lee S K 2009 Covariability of tropical cyclones in the North Atlantic and the eastern North Pacific *Geophys. Res. Lett.* **36** L24702

Wang C and Lee S K 2010 Is hurricane activity in one basin tied to another? *EOS* **91** 93–5